Wave-induced set-up and flow over shoals and coral reefs. Part 1. A simplified bottom geometry case

OCEANOLOGIA, 43 (4), 2001.
pp. 373–388.

KEYWORDS
Wave motion
Set-up
Water flow
Coral reefs
Underwater shoals

Stanisław R. Massel
Institute of Oceanology,
Polish Academy of Sciences,
Powstańców Warszawy 55, PL–81–712 Sopot, Poland;
e-mail: smas@iopan.gda.pl

Richard M. Brinkman
Australian Institute of Marine Science,
Townsville, Qld 4810, Australia

Manuscript received 13 November 2001, reviewed 19 November 2001, accepted 21 November 2001.

Abstract

An analytical approach was used to model the wave-induced set-up and flow through simple shoal geometry when water depth is a linear function of the distance. Two different approaches were applied to parameterize the energy dissipation due to wave breaking. The resulting set-up height and flow velocity were determined and their dependence on the geometry of the shoal and offshore forcing was demonstrated. The extension of the solution to a more complicated bathymetry and verification against the experimental data will be given in the second part of the paper.

1. Introduction

Wave motion is one of the most important dynamic factors determining the hydrodynamics, morphology and biological variability of shallow, submerged coral reefs. Submerged shoals can be found along many ocean coasts. In Europe, such shoals are present along Norwegian, Swedish and

Greek coasts. The water depth at the shoal top is usually very small, but it increases rapidly out of shoal (Lie & Torum 1991). In the tropical regions the most important forms of submerged shoals are coral reefs. Such reefs are common throughout the Pacific, Indian and Atlantic Oceans in the form of fringing reefs surrounding islands, barrier reefs or separate atolls (Veron 1986, Massel 1999).

Shoals and fringing coral reefs act in a similar way to offshore breakwaters and protect shallow lagoonal areas from the full force of oceanic waves. Waves which propagate over the reef slope and are transformed on the shoal or reef platform impose forces on man-made structures and on the organisms inhabiting these areas. In general, there are three processes which dominate the hydrodynamics of shoals and reefs, namely: wave shoaling and breaking, wave set-up and wave-induced flow. In particular, many experimental studies (see for example Hearn & Parker (1988), Wolanski et al. (1993), Gourlay (1994, 1996), Hardy & Young (1996), Kraines et al. (1998), and Massel & Brinkman (1999)) have shown that currents induced by wave breaking and pumping over the shoal top exert a significant impact on the circulation and flushing of the lagoon behind the shoal or coral reef. The continual outflow of water from the lagoon, independently of tidal phase, would indicate that wave pumping is an even more important process than the periodic, tidally driven circulation in reef flushing.

Wave breaking and wave set-up over coral reefs and shoals, recently reported by Massel (1993) and Massel & Gourlay (2000), have been modelled using the extended refraction-diffraction equation for surface waves and the radiation stress concept. However, a solution of this type is valid only for fringing reefs and shoals bounded by coasts not permitting flow through shoals. In such a case, the gradient of the set-up is balanced through the surf zone by the gradient of the radiation stress. For shoals and offshore reefs with a lagoon behind them a wave driven current is generated. To account for this current, a more complete theoretical treatment is required, which incorporates wave breaking, set-up and flow generation.

In this paper, which can be considered as the first part of a more extensive paper, we discuss the set-up and wave-driven flow over an idealized elongated shoal, when the bottom profile can be approximated by the set of linear functions of the distance. Such simplified shoal geometry permits an analytical solution which, however, includes all the basic physical mechanisms of these phenomena. Moreover, this solution provides the opportunity to detect the influence of the particular factors on the final results. The proposed solution is similar to the procedure proposed by Symonds et al. (1995), but has been substantially extended. In particular, in this paper the more complex shape of the offshore shoal is considered.

Instead of the simple similarity model of breaking (the breaking wave height is proportional to the water depth) used by Symonds et al. (1995), the more sophisticated model by Dally et al. (1985) is applied and the wave parameters at the shoal are related to the incident wave parameters in deep water.

This paper is organized as follows. Firstly, the governing equations of the problem and basic assumptions of the model are formulated. Secondly, the solutions are given for the particular regions of the shoal. Thirdly, the matching conditions are explored and the necessary coefficients of the solution are found. Fourthly, the numerical examples are discussed, and finally, in section six, the major conclusions are formulated. The extension of the solution to a more complicated bathymetry and the verification against the experimental data will be given in the second part of the paper, which is in preparation. In particular, the experimental data (Massel & Brinkman, 1999) collected during the field experiment at the Ningaloo Reef (Western Australia) will be used.

2. Governing equations

Consider an elongated offshore shoal or coral reef of simplified cross-section as shown in Fig. 1. Let the origin of a rectangular two-dimensional coordinate system (O, x, z) be taken in the mean free surface of the fluid and the axes be chosen so that the x – coordinate is horizontal and the z – coordinate is vertical and increasing upwards. In the front of the shoal and behind it the water depths are constant and equal to h_0 and h_b, respectively. A plane regular wave train of height H_0 and frequency ω arrives normal to the shoal axis; thus, the problem can be treated as two-dimensional. It is assumed that even at low tide, the shoal top is not exposed and is always covered by water. A wave approaching the shoal transforms over the slope and breaks, inducing set-up of the mean water level and flow over the

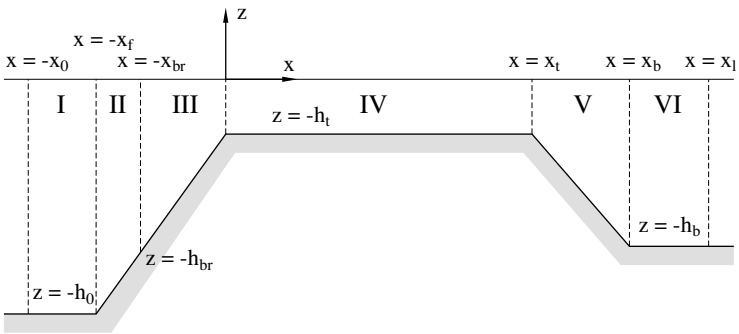

Fig. 1. Diagrammatic shoal defining the parameters used in the theoretical model

shoal top. Let us assume for simplicity that the wave motion is stationary. Moreover, the term $U\frac{dU}{dx}$ is treated as negligibly small when compared with other terms in the momentum equation. As the water depth above the shoal top is small, the water velocity may be represented by its mean value. Therefore, the resulting system of the governing equations can be written as follows (Massel 1989):

$$\frac{d\left[U(x)(h(x)+\bar{\zeta}(x))\right]}{dx}=0, \tag{1}$$

$$0=-g\frac{d\bar{\zeta}(x)}{dx}-\frac{1}{\rho[h(x)+\bar{\zeta}(x)]}\frac{dS_{xx}(x)}{dx}-\frac{\tau_b(x)}{\rho[h(x)+\bar{\zeta}(x)]}, \tag{2}$$

where $h(x)$ is the initial water depth changing in the x – direction, $\bar{\zeta}(x)$ is the wave-driven set-up, $S_{xx}(x)$ is the component of the radiation stress tensor, $\tau_b(x)$ is the bottom friction, ρ is the water density, and $U(x)$ is the depth-integrated velocity, i.e.

$$U(x)=\frac{1}{h(x)+\bar{\zeta}(x)}\overline{\int_{-h(x)}^{\zeta(x)}u(x,z)dz}. \tag{3}$$

To simplify the solution of eqs. (1) and (2), the linear friction law at the sea bottom is applied, i.e.

$$\tau_b(x)=\frac{1}{2}c_f\rho\mid u_w\mid U(x), \tag{4}$$

in which u_w is the wave orbital velocity at the sea bottom and the friction factor c_f has a value from 0.1 to 0.2 for the coral reefs colonized by various types of corals (Nelson 1996), and is of the order 0.01 for sandy bottoms (Longuet-Higgins 1970).

Substituting eq. (4) into eq. (2) we rewrite it in the form demonstrating the partition of the momentum induced by the radiation stress gradient between the pressure gradient and cross-shoal flow

$$[h(x)+\bar{\zeta}(x)]\frac{d\bar{\zeta}(x)}{dx}+\frac{1}{2g}c_f\mid u_w\mid U(x)=-\frac{1}{\rho g}\frac{dS_{xx}(x)}{dx}. \tag{5}$$

Prior to finding an analytical solution to the problem, the following assumptions are made:

- the wave set-up is much smaller than the local water depth, so $h(x)+\bar{\zeta}(x)\approx h(x)$. This assumption is justified by the fact that even in the case of waves propagating over a sloping beach when no flow is permitted, the maximum set-up is only a small portion of the wave height at the breaking point. In the case of the shoal in question with permitted flow, the set-up is even smaller. Eq. (5) therefore becomes

$$h(x)\frac{d\bar{\zeta}(x)}{dx}+\frac{1}{2g}c_f\mid u_w\mid U(x)=-\frac{1}{\rho g}\frac{dS_{xx}(x)}{dx}, \tag{6}$$

- the solution should allow sea level to return to a still water level at a sufficient distance either side of the shoal or reef. Thus, the set-up should vanish at some distances $x = -x_0$ and $x = x_l$, i.e.

$$\bar{\zeta}(x) = 0 \qquad \text{at} \qquad x = -x_0 \tag{7}$$

and

$$\bar{\zeta}(x) = 0 \qquad \text{at} \qquad x = x_l, \tag{8}$$

- a characteristic value of the bottom-wave induced orbital velocity was assumed for simplicity to be constant and equal to the average velocity at the breaking point ($x = -x_{br}$) and shoal edge ($x = 0$), i.e.

$$\mid u_w \mid = \frac{1}{2}\left[u(x = -x_{br}) + u(x = 0)\right]. \tag{9}$$

In each case, the velocity is calculated using a linear wave theory:

$$u(x) = \frac{gkH}{2\omega}\frac{1}{\cosh(kh)}, \tag{10}$$

- seaward of the surf zone we ignore the wave shoaling and assume that the gradient of the radiation stress is zero (see Regions I and II in Fig. 1).

Taking into account the above assumptions, the combination of eqs. (1) and (6) gives the basic equation for the set-up $\bar{\zeta}$ in the form

$$\frac{d^2\bar{\zeta}(x)}{dx^2} + R(x)\frac{d\bar{\zeta}(x)}{dx} + Q(x) = 0, \tag{11}$$

in which

$$R(x) = \frac{2}{h(x)}\frac{dh(x)}{dx}, \tag{12}$$

and

$$Q(x) = -\frac{1}{h(x)}\left(\frac{dF(x)}{dx} + \frac{F(x)}{h(x)}\frac{dh(x)}{dx}\right), \tag{13}$$

$$F(x) = -\frac{1}{\rho g}\frac{dS_{xx}}{dx}. \tag{14}$$

For a given set-up value, the velocity $U(x)$ can be found from eq. (6) in the form

$$U(x) = \frac{F(x)}{r_*} - \frac{h(x)}{r_*}\frac{d\bar{\zeta}(x)}{dx}, \tag{15}$$

in which

$$r_* = \frac{c_f \mid u_w \mid}{2g}. \tag{16}$$

Eq. (11) indicates that the set-up $\zeta(x)$ does not depend on the friction coefficient r_*. This is because the linear friction law is used in the momentum

balance equation (6). However, the current velocity $U(x)$ is affected by the r_* value (see eq. (15)).

3. Solution of eq. (11)

The solution of eq. (11) may be constructed from the particular solutions in each region of the fluid domain. Then the solutions are matched using the conditions which provide continuity of set-up and velocity at the cross-sections $x = -x_f$, $x = -x_{br}$, $x = 0$, $x = x_t$ and $x = x_b$.

Region I – constant water depth area in front of the shoal $(-x_0 < x < -x_f,\ z = -h_0)$

In the absence of wave breaking and bottom friction, the radiation stress gradient $\frac{dS_{xx}}{dx}$ vanishes. Therefore, $F(x) = Q(x) = 0$ and eq. (11) takes the form

$$\frac{d^2\bar{\zeta}(x)}{dx^2} = 0, \tag{17}$$

with the solution

$$\bar{\zeta}(x) = C_1 + C_2(x + x_0) \qquad \text{and} \qquad U(x) = -\frac{C_2\, h_0}{r_*}. \tag{18}$$

Region II – seawards breaking line $(-x_f < x < -x_{br},\ -h_0 < z < h_{br})$

The radiation stress gradient $\frac{dS_{xx}}{dx}$ is negligibly small in this Region. Thus, assuming that $F(x) = 0$ and $Q(x) = 0$, we get from eq. (11)

$$\frac{d^2\bar{\zeta}(x)}{dx^2} - \frac{2m}{h(x)}\frac{d\bar{\zeta}(x)}{dx} = 0, \tag{19}$$

where $h(x) = h_t - mx$ and m is the seaward bottom slope of the shoal. The solution of eq. (19) becomes

$$\bar{\zeta}(x) = \frac{-C_3}{h_t - mx} + C_4 \qquad \text{and} \qquad U = \frac{mC_3}{r_*\,(h_t - mx)}. \tag{20}$$

Region III – surf zone $(-x_{br} < x < 0,\ -h_{br} < z < 0)$

We assume that at water depth h_{br} the wave starts to break. In order to determine the breaking point and water depth at breaking, we first parameterize the breaking wave height using a formula proposed by Singamsetti and Wind (1980):

$$H_{br} = 0.575\, m^{0.031} \left(\frac{H_\infty}{L_\infty}\right)^{-0.254} H_\infty, \tag{21}$$

in which L_∞ is the deep water wave length, i.e. $L_\infty = \frac{2\pi g}{\omega^2}$. For the non-dimensional wave height $\left(\frac{H}{h}\right)_{br}$ we have

$$\left(\frac{H}{h}\right)_{br} = 0.937\, m^{0.155} \left(\frac{H_\infty}{L_\infty}\right)^{-0.130}. \tag{22}$$

Combining eqs. (21) and (22) we get

$$h_{br} = 0.614 m^{-0.124} \left(\frac{H_\infty}{L_\infty}\right)^{-0.124} H_\infty, \tag{23}$$

and

$$x_{br} = -\frac{h_{br} - h_t}{m}. \tag{24}$$

As the incident wave parameters are given for the water depth h_0, we have to estimate the deep water wave height H_∞ and the wavelength L_∞ using the reversed refraction approach. Thus, we have (Massel 1989)

$$H_\infty = \sqrt{\frac{C_{g0}}{C_{g\infty}}} H_0, \tag{25}$$

where C_{g0} and $C_{g\infty}$ are the group velocities at the water depth h_0 and in the deep sea ($h = \infty$), respectively, i.e.

$$C_{g\infty} = \frac{1}{2}\frac{g}{\omega} \tag{26}$$

and

$$C_{g0} = \frac{1}{2}\left(1 + \frac{2k_0h_0}{\sinh(2k_0h_0)}\right)\sqrt{\frac{g}{k_0}\tanh(k_0h_0)}, \tag{27}$$

in which the wave number k_0 is a solution of the dispersion relation

$$\omega = \sqrt{gk_0 \tanh(k_0h_0)}. \tag{28}$$

Depending on the energy of the incident waves and the bottom slope, wave breaking can be restricted to Region III, or it can continue in Region IV. To find the corresponding set-up value in Region III we first determine the radiation stress S_{xx}, assuming shallow water and a normal wave approach. Thus, we have (Massel 1989)

$$S_{xx} = \frac{3}{16}\rho g H^2(x). \tag{29}$$

In the literature there are a few procedures available for modelling the variation of wave height $H(x)$ over coastal slopes (for more details, see for example Massel 1996a). For our purpose we apply the intuitive model developed by Dally et al. (1985) in which a wave attenuates over the uniform slope as follows:

$$H^2(x) = \left[\left(\frac{h(x)}{h_{br}}\right)^\beta (1+\alpha) - \alpha\left(\frac{h(x)}{h_{br}}\right)^2\right] H_{br}^2, \tag{30}$$

in which

$$\alpha = \frac{K\Gamma_3^2}{m\left(\frac{5}{2} - \frac{K}{m}\right)}\left(\frac{H_{br}}{h_{br}}\right)^{-2} \qquad \text{and} \qquad \beta = \frac{K}{m} - \frac{1}{2}, \tag{31}$$

in which the water depth $h(x) = h_t - mx$, K is a dimensionless decay coefficient and Γ_3 is a dimensionless stable wave coefficient for a sloping bottom. The coefficients K and Γ_3 control the attenuation of wave energy until a stable wave height ($H \approx \Gamma_3\, h(x)$) is attained. According to Dally et al. (1985), the value of K appears somewhere between 0.100 and 0.275, and for Γ_3, the range of applicability is from about 0.35 to 0.50. However, these estimates are proposed for shoal slopes of the range from 1/80 to 1/30. For steeper slopes, the values of K and Γ_3 are still not known.

Using eq. (30) we get the following solution of the basic equation (eq. (11))

$$\bar{\zeta}(x) = \frac{C_5}{mh(x)} - \frac{A}{m^2\beta(\beta-1)}[h(x)]^{\beta-1} + \frac{B}{2m}x + C_6, \tag{32}$$

and for velocity $U(x)$ we obtain

$$\begin{aligned} U(x) &= \frac{1}{r_*}\frac{3mH_{br}}{16}\left(\frac{H_{br}}{h_{br}}\right)\left[\beta(1+\alpha)\left(\frac{h(x)}{h_{br}}\right)^{\beta-1} - 2\alpha\left(\frac{h(x)}{h_{br}}\right)\right] \\ &- \frac{h(x)}{r_*}\left[C_5[h(x)]^{-2} + \frac{A}{m\beta}[h(x)]^{\beta-2} + \frac{B}{2m}\right], \end{aligned} \tag{33}$$

in which

$$A = \frac{3m^2}{16}\left(\frac{H_{br}}{h_{br}}\right)^2 \frac{\beta^2(1+\alpha)}{h_{br}^{\beta-2}}, \tag{34}$$

$$B = \frac{-3m^2}{4}\left(\frac{H_{br}}{h_{br}}\right)^2 \alpha. \tag{35}$$

Eq. (32) indicates that this solution is not valid for $\beta = 0\,(K = \frac{m}{2})$ and $\beta = 1(K = \frac{3m}{2})$. However, after the reformulation of the above equations, it can be found that for $\beta = 0$, the solution of eq. (11) becomes

$$\bar{\zeta}(x) = \frac{C_5}{mh(x)} + \frac{B}{2m}x + C_6, \tag{36}$$

and

$$U(x) = -\frac{1}{r_*}\frac{3m\alpha}{8}\left(\frac{H_{br}}{h_{br}}\right)\left(\frac{h(x)}{h_{br}}\right)H_{br} - \frac{h(x)}{r_*}\left[\frac{C_5}{[h(x)]^2} + \frac{B}{2m}\right]. \tag{37}$$

Similarly, when $\beta = 1$, we obtain

$$\bar{\zeta}(x) = \frac{C_5}{mh(x)} - \frac{A}{m^2}\ln[h(x)] + \frac{B}{2m}x + C_6, \tag{38}$$

and

$$U(x) = \frac{1}{r_*}\frac{3mH_{br}}{16}\left(\frac{H_{br}}{h_{br}}\right)\left[(1+\alpha) - 2\alpha\left(\frac{h(x)}{h_{br}}\right)\right] - \frac{h(x)}{r_*}\left[\frac{C_5}{[h(x)]^2} + \frac{A}{mh(x)} + \frac{B}{2m}\right]. \quad (39)$$

The case when $\frac{K}{m} = \frac{5}{2}(\alpha = \infty)$ requires a special analysis which will not be given here.

It should be noted that when $\alpha = -1$, eq. (30) reverts to the common similarity model when

$$H(x) = \left(\frac{H_{br}}{h_{br}}\right)h(x) = \gamma h(x), \quad (40)$$

where γ is the breaking factor. After substituting $\alpha = -1$ into eqs. (32) and (33), we get

$$\bar{\zeta}(x) = \frac{C_5}{mh(x)} + \frac{B}{2m}x + C_6 \qquad \text{and} \qquad U(x) = -\frac{C_5}{r_* h(x)}. \quad (41)$$

Region IV – shoal top ($0 < x < x_t$, $z = -h_t$)

To find the set-up value over the shoal top, we consider two scenarios. In the first we assume that the breaking process is totally confined within Region III. Thus, at the edge ($x = 0$), the wave is stable and its height is smaller than the critical value corresponding to the constant water depth, i.e. $H(0) < \Gamma_4 h_t$, where Γ_4 is a dimensionless stable wave height coefficient for $h_t = \text{const}$. To estimate the maximum non-breaking wave height in Region IV, we use the results of the extended experimental data summarized by Nelson (1994) and Massel (1996b). These results suggest that the dimensionless stable wave coefficient Γ_4 can be expressed as follows:

$$\Gamma_4 = \left[\frac{\sqrt{1 + 0.01504h_*^{-2.5}} - 1}{0.1654h_*^{-1.25}}\right]^2, \quad (42)$$

in which

$$h_* = \frac{h_t}{gT^2}. \quad (43)$$

In the second scenario, the wave breaking process continues in Region IV, over the shoal top as the wave height $H(0) > \Gamma_4 h_t$. Therefore, the wave height is still decreasing from its initial value $H(0)$ until a stable condition is reached at some distance from the shoal edge.

Let us consider first the case when $H(0) > \Gamma_4 h_t$, and the gradient of the wave height and radiation stress are not zero. For consistency we represent

the variation of the wave height $H(x)$ over the constant water depth by the Dally et al. (1985) model also, i.e.

$$H^2(x) = \left\{ \left[\left(\left(\frac{H(0)}{h_t} \right)^2 - \Gamma_4^2 \right) \exp\left(-K \frac{x}{h_t} \right) \right] + \Gamma_4^2 \right\} h_t^2. \tag{44}$$

The corresponding solution of eq. (11) becomes

$$\bar{\zeta}(x) = C_7 x - M \exp\left(-K \frac{x}{h_t} \right) + C_8 \qquad \text{and} \qquad U(x) = -\frac{C_7 h_t}{r_*}, \tag{45}$$

where

$$M = \frac{3}{16} G h_t, \tag{46}$$

and

$$G = \left(\frac{H(0)}{h_t} \right)^2 - \Gamma_4^2. \tag{47}$$

For a stable regime, when $H(0) < \Gamma h_t$, waves do not break ($K = 0$). Therefore, for a constant water depth, the radiation stress gradient vanishes, i.e. $F = 0$ and eq. (11) has the solution

$$\bar{\zeta}(x) = C_7\, x + C_8 \qquad \text{and} \qquad U = -\frac{C_7\, h_t}{r_*}. \tag{48}$$

Region V – shoreward slope of shoal ($x_t < x < x_b$, $-h_b < z < -h_t$)

Similarly to Region II, eq. (11) becomes

$$\frac{d^2\bar{\zeta}}{dx^2} + \frac{2m_1}{h(x)} \frac{d\bar{\zeta}}{dx} = 0, \tag{49}$$

in which $h(x) = h_t + m_1(x - x_t)$ and m_1 is the slope of the backward slope of the shoal. The solution of eq. (49) is

$$\bar{\zeta}(x) = \frac{-C_9}{[h_t + m_1(x - x_t)]} + C_{10} \text{ and } U(x) = \frac{-m_1 C_9}{r_*[h_t + m_1(x - x_t)]}. \tag{50}$$

Region VI – lagoon behind shoal ($x_b < x < x_l$, $z = -h_b$)

The water depth in the lagoon is assumed constant. Therefore, no gradient of the radiation stress S_{xx} exists. Thus, $F = \frac{dF}{dx} = 0$ and the solution of eq. (11) becomes

$$\bar{\zeta}(x) = C_{11}\,(x_l - x) + C_{12} \qquad \text{and} \qquad U = \frac{C_{11}\, h_b}{r_*}. \tag{51}$$

The constants C_1,....,C_{12} are determined from the boundary conditions (7) and (8), and the continuity of the set-up and velocity at the cross-sections $x = x_f$, $x = x_{br}$, $x = 0$, $x = x_t$ and $x = x_b$. The resulting expressions for coefficients C_n are listed in the Appendix.

4. Numerical calculations

In the previous Sections, a closed-form solution was obtained for the simpler case of wave breaking on the shoals of the idealized plane bottom shapes. Using this solution, Fig. 2 shows the resulting set-up, current velocity and cross shoal transport for a shoal of 1:25 seawards and shoreward slopes. The gradient of the radiation stress through the surf zone and shoal top produces the set-up and accelerates a current up the slope. Maximum set-up is about 10% of the incident wave height. The current velocity over the shoal top is constant to match the continuity of the cross shoal transport which is calculated as a product of flow velocity and water depth.

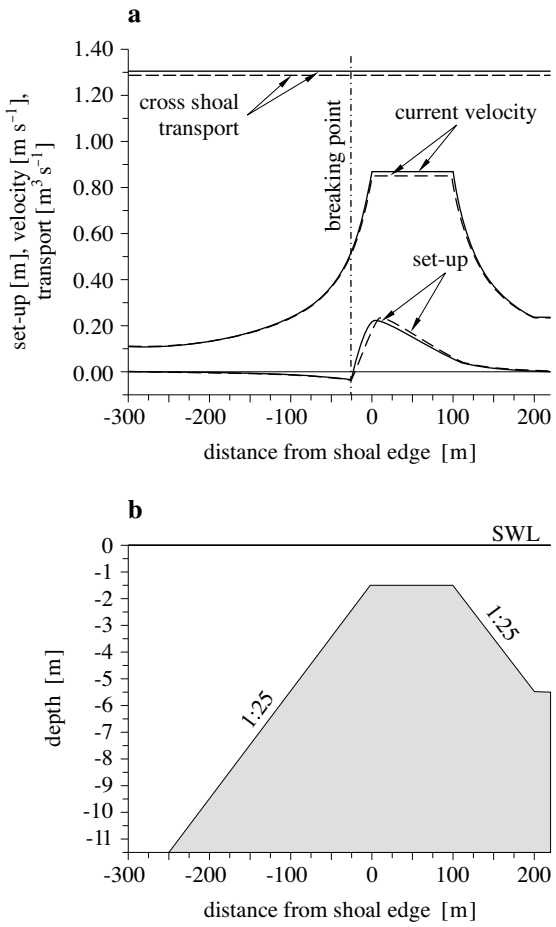

Fig. 2. Wave impact on the shoal ($H_0 = 2m$, $T = 4s$, $K = 0.275$, $\Gamma = 0.475$): wave set-up, induced flow and cross shoal transport (a); geometry of a shoal with lagoon behind (b). Solid line – solution using the dissipation model by Dally et al., dashed line – solution using the similarity dissipation model

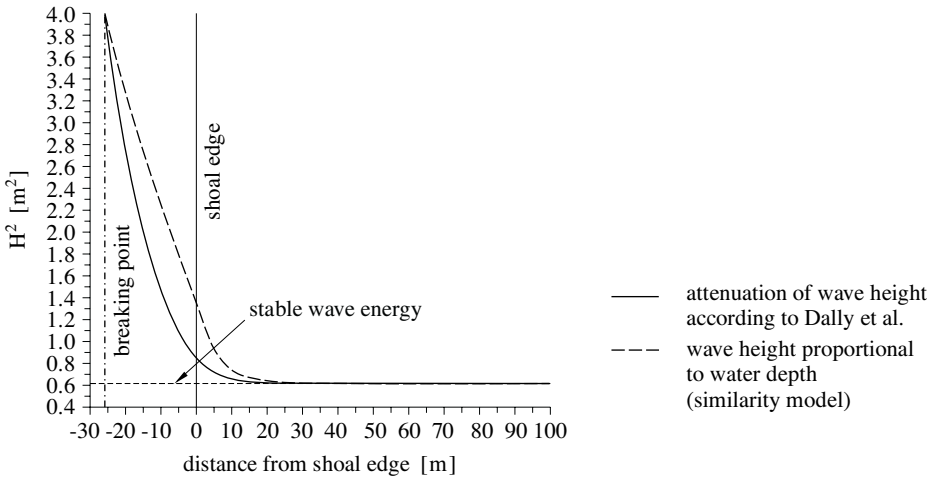

Fig. 3. Wave energy attenuation according to Dally et al. and similarity models

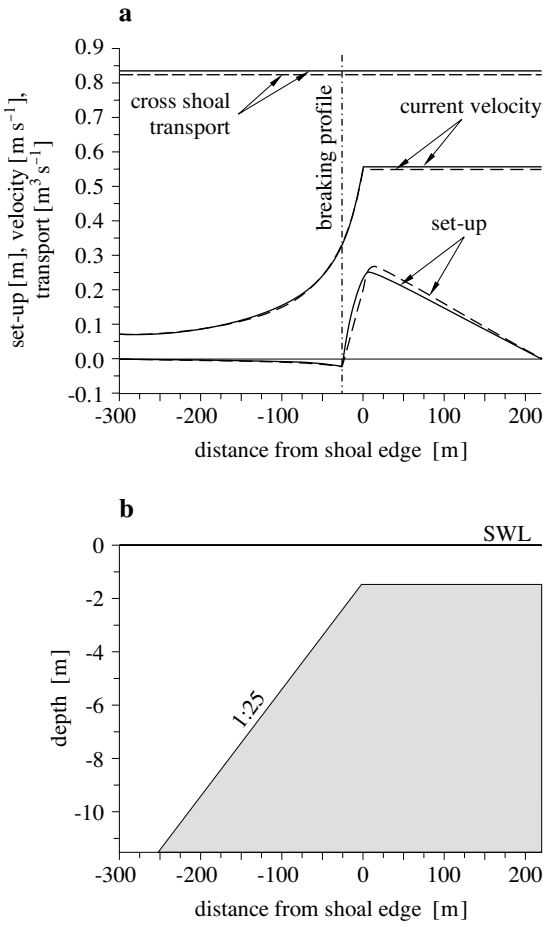

Fig. 4. Wave impact on the shoal ($H_0 = 2m, T = 4s$ $K = 0.275$, $\Gamma = 0.475$): wave set-up, induced flow and cross shoal transport (a); wide flat shoal geometry (b). Dashed line – solution using the similarity dissipation model

It should be noted that the set-down value observed at the breaking point is not associated with wave shoaling as predicted by Longuet-Higgins & Stewart (1964), because we assumed that the radiation stress gradient is negligibly small in the Regions seaward of the surf zone (Regions I and II). The set-down shown in Fig. 2 results from the pressure gradient needed to produce transport through the shoal. Therefore, the set-down value depends on the magnitude of transport. As at the shoal edge, the wave height is greater than the stable value $\Gamma_4 h_t$, the breaking continues in Region IV (constant water depth), where the wave height should satisfy eq. (44).

In the same Figure, results for a common similarity model ($H(x) \approx h(x)$) are shown (dashed lines) for comparison. Under the similarity assumption, the wave height in Region III varies proportionally to the water depth, i.e. $H(x) = \frac{H_{br}}{h_{br}} h(x)$. For given incident wave parameters and shoal geometry, both approaches result in very similar values of the set-up and current velocity. The small differences observed are due to different wave energy attenuation scenarios, which are shown in Fig. 3. In Region III, between breaking point and shoal edge, the gradient of $\frac{dS_{xx}}{dx} \approx \frac{H^2}{dx}$ for the Dally et al. model is greater than for the similarity model. In Region IV, the gradients are opposed.

This solution can be extended to study waves propagating over a wide flat shoal, without a rear slope ($m_1 \to 0$) – (see Fig. 4). Under the same incident wave parameters, the wave set-up value is slightly higher than for the case shown in Fig. 2. As the resulting current velocity is smaller, the set-up attenuates slowly and vanishes at the end of shoal ($x = x_l$) to much

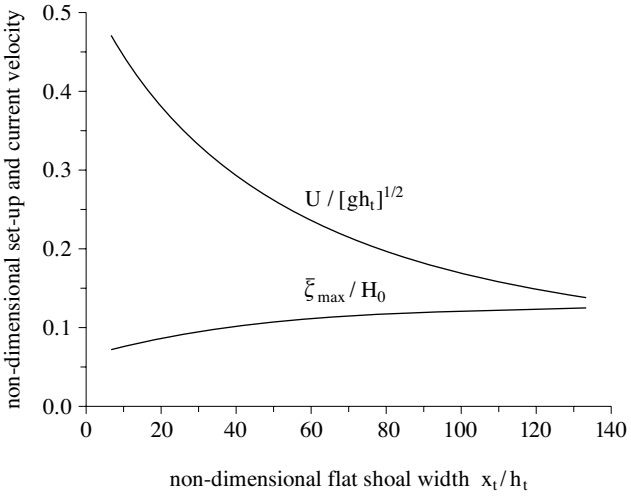

Fig. 5. Relationship between depth-averaged velocity and set-up

the boundary condition (8). Both wave height attenuation scenarios yield a very similar set-up and current velocity values.

Figs. 2 and 4 showed that the magnitudes of the current velocity and set-up depend on the width of the shoal top. This dependence is shown in Fig. 5. The non-dimensional set-up increases when the non-dimensional flat shoal is widening. The opposite tendency is shown for the non-dimensional flow velocity.

5. Conclusions

This paper examines the wave-induced component of cross-shoal flow. A linear model was used for the simple shoal geometry when the depth is a linear function of distance. This assumption permits an analytical solution of the corresponding boundary value problem. Two different approaches have been applied to the parameterization of the dissipation due to wave breaking. Numerical calculations show that there is no great difference between the resulting set-up heights and the flow velocities for the two parameterizations. The model demonstrates how the relative flow velocity and set-up height depend on the geometry of the shoal and offshore forcing.

The extension of the solution to a more complicated bathymetry and the verification against the experimental data collected during the field experiment at the Ningaloo Reef (Western Australia) will be given in the second part of the paper, which is in preparation.

References

Dally W. R., Dean R. G., Dalrymple R. A., 1985, *Wave height variation across beaches of arbitrary profile*, J. Geophys. Res., 90, 11917–11927.

Gourlay M. R., 1994, *Wave transformation on a coral reef*, Coast. Eng., 23, 17–42.

Gourlay M. R., 1996, *Wave set-up on coral reefs: 1. Set-up and wave-generated flow on an idealized two dimensional horizontal reef*, Coast. Eng., 27, 161–193.

Hardy T. A., Young I. R., 1996, *Field study of wave attenuation on an offshore coral reef*, J. Geophys. Res., 101, 14311–14326.

Hearn C. J., Parker I. N., 1988, *Hydrodynamic processes on the Ningaloo Reef, Western Australia*, Proc. 6th Int. Symp. Coral Reefs, 2, 497–502.

Kraines S. B., Yanagi T., Isobe M., Komiyama H., 1998, *Wind-wave driven circulation on the coral reef at Bora Bay, Miyako Island*, Coral Reefs, 17, 133–143.

Lie V., Torum A., 1991, *Ocean waves over shoals*, Coast. Eng., 15, 545–562.

Longuet-Higgins M. S., 1970, *Longshore currents generated by obliquely incident sea waves*, J. Geophys. Res., 75, 6790–6801.

Longuet-Higgins M. S., Stewart R. W., 1964, *Radiation stresses in water waves; a physical discussion with applications*, Deep-Sea Res., 11, 529–562.

Massel S. R., 1989, *Hydrodynamics of coastal zones*, Elsevier, Amsterdam, 336 pp.

Massel S. R., 1993, *Extended refraction-diffraction equation for surface waves*, Coast. Eng., 19, 97–126.

Massel S. R., 1996a, *Ocean surface waves: their physics and prediction*, World Sci. Publ., Singapore–London–Hong Kong, 491 pp.

Massel S. R., 1996b, *On the largest wave height in water of constant depth*, Ocean Eng., 23, 553–573.

Massel S. R., 1999, *Fluid mechanics for marine ecologists*, Springer Verlag, Heidelberg–Berlin, 566 pp.

Massel S. R., Brinkman R. M., 1999, *Measurement and modelling of wave propagation and breaking at steep coral reefs*, [in:] *Recent advances in marine science and technology '98*, N. K. Saxena (ed.), PACON Int., Honolulu, 27–36.

Massel S. R., Gourlay M. R., 2000, *On the modelling of wave breaking and set-up on coral reefs*, Coast. Eng., 39, 1–27.

Nelson R. C., 1994, *Depth limited design wave heights in very flat regions*, Coast. Eng., 23, 43–59.

Nelson R. C., 1996, *Hydraulic roughness of coral reef platforms*, Appl. Ocean Res., 18, 265–274.

Singamsetti S. R., Wind E. G., 1980, *Breaking waves: characteristics of shoaling and breaking periodic waves normally incident to plane beaches of constant slope*, Delft Hydr. Lab., Rep. M1371, 80 pp.

Symonds G., Black K. P., Young I. R., 1995, *Wave-driven flow over shallow reefs*, J. Geophys. Res., 100, 2639–2648.

Veron J. E. N., 1986, *Corals of Australia and the Indo-Pacific*, Univ. Hawaii Press, Honolulu, 644 pp.

Wolanski E., Delesalle B., Dufour V., Aubanel A., 1993, *Modeling the fate of pollutants in the Tiahura Lagoon, Moorea, French Polynesia*, Proc. 11th Austr. Coast. Ocean Eng. Conf., Townsville, 1, 583–589.

Appendix – Coefficients C_n and p_n

Boundary conditions (7) and (8) and the continuity of the set-up and velocity at the cross-sections $x = x_f$, $x = x_{br}$, $x = 0$, $x = x_t$ and $x = x_b$ give the following relationships for the coefficients C_n:

$$C_1 = 0 \qquad \text{and} \qquad C_2 = p_{211}C_{11} + p_{200}, \tag{52}$$

$$C_3 = p_{311}C_{11} + p_{300} \qquad \text{and} \qquad C_4 = p_{411}C_{11} + p_{400}, \tag{53}$$

$$C_5 = p_{511}C_{11} + p_{501} \qquad \text{and} \qquad C_6 = p_{611}C_{11} + p_{600}, \tag{54}$$

$$C_7 = p_{711}C_{11} \qquad \text{and} \qquad C_8 = p_{811}C_{11} + p_{800}, \tag{55}$$

$$C_9 = p_{911}C_{11} \qquad \text{and} \qquad C_{10} = p_{1011}C_{11}, \tag{56}$$

$$C_{11} = \frac{p_{11a}}{p11b} \qquad \text{and} \qquad C_{12} = 0, \tag{57}$$

in which

$$p_{711} = -\left(\frac{h_b}{h_t}\right)^2 \qquad \text{and} \qquad p_{911} = -\frac{h_b^2}{m_1}, \tag{58}$$

$$p_{1011} = (x_l - x_b) - \frac{h_b}{m_1} \qquad \text{and} \qquad p_{800} = M\exp\left(-K\frac{x_t}{h_t}\right), \tag{59}$$

$$p_{811} = p_{1011} - \frac{p_{911}}{h_t} - p_{711}\,h_t, \tag{60}$$

$$p_{500} = \frac{3mH_{br}}{16}\left(\frac{H_{br}}{h_{br}}\right)\left[\beta(1+\alpha)\left(\frac{h_t}{h_{br}}\right)^{\beta-1} - 2\alpha\left(\frac{h_t}{h_{br}}\right)\right] \tag{61}$$

$$- \; h_t\left[\frac{A}{m\beta}h_t^{\beta-2} + \frac{B}{2m}\right], \tag{62}$$

$$p_{501} = p_{500}\,h_t \qquad \text{and} \qquad p_{511} = h_t^2\,p_{711}, \tag{63}$$

$$p_{600} = p_{800} - M - \frac{p_{501}}{mh_t} + \frac{A}{m^2\beta(\beta-1)}h_t^{\beta-1}, \tag{64}$$

$$p_{611} = p_{811} - \frac{p_{511}}{mh_t}, \tag{65}$$

$$p_{301} = \frac{3mH_{br}}{16}\left(\frac{H_{br}}{h_{br}}\right)[\beta(1+\alpha) - 2\alpha] - h_{br}\left[\frac{A}{m\beta}h_{br}^{\beta-2} + \frac{B}{2m}\right], \tag{66}$$

$$p_{300} = \frac{1}{m}\left(p_{301}h_{br} - p_{501}\right) \qquad \text{and} \qquad p_{311} = -\frac{p_{511}}{m}, \tag{67}$$

$$p_{200} = -\frac{m\,p_{300}}{h_0^2} \qquad \text{and} \qquad p_{211} = -\frac{m\,p_{311}}{h_0^2}, \tag{68}$$

$$p_{400} = (x_0 - x_f)p_{200} + \frac{p_{300}}{h_0} \qquad \text{and} \qquad p_{411} = (x_0 - x_f)p_{211} + \frac{p_{311}}{h_0}, \tag{69}$$

$$p_{11a} = \frac{p_{300}}{h_{br}} - p_{400} + \frac{p_{501}}{mh_{br}} + p_{600} - \frac{A}{m^2\beta(\beta-1)}h_{br}^{\beta-1} + \frac{B}{2m}x_{br}, \tag{70}$$

$$p_{11b} = -\frac{p_{311}}{h_{br}} + p_{411} - \frac{p_{511}}{mh_{br}} - p_{611}. \tag{71}$$